

The Plant Cell, Vol. 26: 4519–4531, November 2014, www.plantcell.org © 2014 American Society of Plant Biologists. All rights reserved.

Cellular Metabolites Enhance the Light Sensitivity of *Arabidopsis* Cryptochrome through Alternate Electron Transfer Pathways^{CJW|OPEN}

Christopher Engelhard,^a Xuecong Wang,^b David Robles,^b Julia Moldt,^{c,1} Lars-Oliver Essen,^d Alfred Batschauer,^c Robert Bittl,^a and Margaret Ahmad^{b,e,2}

^aFachbereich Physik, Free University, 14195 Berlin, Germany

^bUniversity of Paris VI, UMR 8256 (B2A), IBPS, 75005 Paris, France

^cDepartment of Plant Physiology and Photobiology, Faculty of Biology, Philipps-University, 35032 Marburg, Germany

^dBiomedical Research Centre/Faculty of Chemistry, Philipps-University, 35032 Marburg, Germany

^eXavier University, Cincinnati, Ohio 45207

Cryptochromes are blue light receptors with multiple signaling roles in plants and animals. Plant cryptochrome (*cry1* and *cry2*) biological activity has been linked to flavin photoreduction via an electron transport chain comprising three evolutionarily conserved tryptophan residues known as the Trp triad. Recently, it has been reported that *cry2* Trp triad mutants, which fail to undergo photoreduction in vitro, nonetheless show biological activity in vivo, raising the possibility of alternate signaling pathways. Here, we show that *Arabidopsis thaliana cry2* proteins containing Trp triad mutations indeed undergo robust photoreduction in living cultured insect cells. UV/Vis and electron paramagnetic resonance spectroscopy resolves the discrepancy between in vivo and in vitro photochemical activity, as small metabolites, including NADPH, NADH, and ATP, were found to promote cry photoreduction even in mutants lacking the classic Trp triad electron transfer chain. These metabolites facilitate alternate electron transfer pathways and increase light-induced radical pair formation. We conclude that cryptochrome activation is consistent with a mechanism of light-induced electron transfer followed by flavin photoreduction in vivo. We further conclude that in vivo modulation by cellular compounds represents a feature of the cryptochrome signaling mechanism that has important consequences for light responsivity and activation.

INTRODUCTION

Cryptochromes are flavoprotein receptors found throughout the biological kingdom that have been implicated in numerous signaling functions (Lin and Todo, 2005; Chaves et al., 2011). In plants, cryptochromes mediate photomorphogenesis and growth responses to blue light, which include inhibition of hypocotyl elongation, regulation of gene expression, the initiation of flowering, and entrainment of the circadian clock (Chaves et al., 2011). Plant *cry2* proteins furthermore undergo ubiquitination subsequent to light activation in vivo, followed by targeting to the proteasome and subsequent degradation (Yu et al., 2009; Weidler et al., 2012). In animal systems, cryptochromes play a central role in the circadian clock in both flies and mammals and have been proposed as possible magnetoreceptors in migratory birds (Chaves et al., 2011).

Structurally and mechanistically, cryptochromes are closely related to photolyases, which are evolutionarily conserved flavoproteins that perform light-dependent redox reactions and repair DNA via electron transfer (Brettel and Byrdin, 2010). Although most cryptochromes do not repair DNA, studies with isolated proteins in vitro have shown that many of the photochemical reactions found in photolyases are also conserved in cryptochromes, including light-induced electron transfer and flavin reduction (Brettel and Byrdin, 2010). It has furthermore been shown that downstream signaling molecules such as CONSTITUTIVE MORPHOGENESIS1 (COP1), SUPPRESSOR OF PHYA-105 (SPA1), and CRYPTOCHROME-INTERACTING BASIC-HELIX-LOOP-HELIX1 (CIB1), which mediate photomorphogenesis and flowering (Yang et al., 2000; Liu et al., 2008; Liu et al., 2011; Zuo et al., 2011; Liu et al., 2013), bind to light-activated *Arabidopsis thaliana* cryptochromes. As a result, the proposed mechanism of cry biological activation is that in the dark, the C-terminal region is folded in such a way as to render the receptor inaccessible to signaling partners and therefore inactive. A photon is absorbed by the N-terminal flavin binding domain and initiates a chemical reaction within the protein, which in turn triggers a conformational change. The resulting “lit” state renders the cryptochrome receptor accessible to interacting proteins that trigger photomorphogenesis and signaling, while at the same time exposing ubiquitination sites elsewhere on the protein that target *cry2* for degradation (Zuo et al., 2011, 2012). The current challenge in this field is to determine which of the

¹ Current address: Institute of Biology, Experimental Biophysics, Humboldt-University Berlin, 10115 Berlin, Germany.

² Address correspondence to margaret.ahmad@upmc.fr.

The author responsible for distribution of materials integral to the findings presented in this article in accordance with the policy described in the Instructions for Authors (www.plantcell.org) is: Margaret Ahmad (margaret.ahmad@upmc.fr).

Some figures in this article are displayed in color online but in black and white in the print edition.

Online version contains Web-only data.

Articles can be viewed online without a subscription.

www.plantcell.org/cgi/doi/10.1105/tpc.114.129809

known primary photoreactions occurring in isolated cryptochromes *in vitro* are required for the initiation of biological activity and photomorphogenesis *in vivo*.

Attention has focused primarily on photoreduction of the flavin adenine dinucleotide (FAD) cofactor as the biologically relevant primary light-sensing step performed by plant (*cry1* and *cry2*) cryptochromes. This process, also known as “photoactivation,” is held in common with ancestral photolyases and involves light-driven electron transfer to an excited state flavin through a chain of three highly conserved Trp amino acid residues known as the Trp triad (Brettel and Byrdin, 2010; Chaves et al., 2011). The resulting transition from oxidized to radical flavin is thought to induce the relevant conformational changes in the protein (Partch et al., 2005; Kondoh et al., 2011), which leads to interaction with signaling partners (Liu et al., 2008; Zuo et al., 2011). Return to darkness results in slow reoxidation of the flavin (over several minutes) causing resetting of the system to the dark (inactive) form. The result is a light-activated biological switch that cycles between active (light-induced) and inactive (dark-adapted) conformations on a time scale (several minutes) consistent with a biologically relevant signaling mechanism (Banerjee et al., 2007; Bouly et al., 2007; Müller and Ahmad, 2011; Burney et al., 2012; Herbel et al., 2013). Similar redox reactions (photoreduction) are shown to occur in animal-type cryptochromes (*Drosophila melanogaster* and human), both *in vivo* and *in vitro* (VanVickle-Chavez and Van Gelder, 2007; Hoang et al., 2008; Vaidya et al., 2013).

There are a number of lines of evidence for photoreduction as a mechanism for *cry* activation *in vivo*. First, the Trp triad is conserved in most plant and animal type cryptochromes that have been sequenced, and mutational analysis has demonstrated that this electron transfer pathway is functional during the photoreduction of isolated plant *cry1* and *cry2* cryptochromes (Zeugner et al., 2005; Banerjee et al., 2007; Bouly et al., 2007). Second, unlike in photolyases, the dark resting state of flavin in plant cryptochromes is the oxidized redox state *in vivo* (Ahmad et al., 2002; Banerjee et al., 2007; Bouly et al., 2007; Balland et al., 2009), which can be photoreduced by light. Third, illumination of whole living insect cells expressing recombinant *Arabidopsis cry1* or *cry2* demonstrated that flavin photoreduction and radical accumulation occurs *in vivo* (Banerjee et al., 2007; Bouly et al., 2007). Fourth, studies in planta have shown that light treatments that diminish the pools of *cry* radical (for instance green light irradiation) result in diminished cryptochrome activity in photomorphogenesis, the initiation of flowering, or degradation of *cry2* (Banerjee et al., 2007; Bouly et al., 2007). Fifth, mutations that fail to undergo photoreduction do not undergo conformational change *in vitro* (Kondoh et al., 2011) and show reduced biological function in photomorphogenesis in planta (Zeugner et al., 2005). Sixth, the *in vivo* lifetime of the *cry* signaling state correlates well with the lifetime of the flavin radical state (Herbel et al., 2013). A mechanism has therefore been proposed whereby light-driven *cry* photoreduction leads ultimately to change from an inactive to active conformational state that is accessible for interaction with downstream signaling partners (COP1, CIB1, and SPA1). This active signaling state is restored to the inactive (resting) state upon return to darkness by a process of reoxidation involving molecular oxygen (Müller

and Ahmad, 2011). Thus, light-driven cycling between alternate redox states has been proposed to explain the evolution from photolyase to cryptochromes and the basis for signaling in plant (Burney et al., 2012) and also animal cryptochromes (Hoang et al., 2008; Vaidya et al., 2013).

This proposed mechanism has come under discussion in a number of studies from *Drosophila Cry* (Song et al., 2007; Öztürk et al., 2008; Öztürk et al., 2011, 2014) and *Arabidopsis cry2* (Li et al., 2011). These studies in common showed that mutations in the Trp triad result in decreased cryptochrome flavin reduction *in vitro* but did not seem to eliminate biological activity *in vivo*. For example, Trp triad mutants of *Arabidopsis cry2* (Li et al., 2011), namely, W321A, W374A, and W397A, retained responsiveness to blue light in a reporter assay that monitored their blue light-induced proteolysis in expressing transgenic plants (Li et al., 2011). Such *cry2* degradation results from ubiquitination of the receptor in the light-activated form followed by targeting to the proteasome and is widely accepted as a readout for *cry2* activation in planta (Yu et al., 2009; Weidler et al., 2012). In particular, the mutant W374A showed a light response approaching that of the wild-type *cry2* *in vivo*, even though the isolated W374A protein *in vitro* did not undergo significant photoreduction (Li et al., 2011). Therefore, the role of photoreduction as a means of activating cryptochromes has been disputed. This raised the important question of how such mutants, in which the isolated proteins showed no significant photoreduction (light activation) *in vitro*, could nevertheless be light responsive in transgenic plants *in vivo*.

In this work, we resolve this seeming discrepancy between *in vitro* photoreactions and reported *in vivo* biological activity for *Arabidopsis cry2* by determining the photoreactions (light responses) that occur in cryptochrome within living cells. We show by UV/Vis and electron paramagnetic resonance (EPR) spectroscopic techniques that the substitution mutations W321A, W321F, W374A, W374F, and W397A undergo robust light-dependent photoreduction in an *in vivo* context, in marked contrast to the isolated proteins. This led to the discovery that small molecule activators including ATP, NADH, and NADPH profoundly modulate cryptochrome activity *in vivo* by facilitating the use of alternate electron transfer pathways. We conclude that reported *in vivo* biological activation of cryptochromes in the course of plant growth and development is fully consistent with electron transfer to flavin as a light sensing mechanism and involves both the Trp triad and alternative electron transfer pathways. We further conclude that *cry* photochemistry and ultimate biological activity is modulated to an unprecedented degree by chemical mechanisms that may be evolutionarily conserved and could provide the basis for novel pharmacological intervention in *cry* function.

RESULTS

Photoactivation and Flavin Radical Formation *In Vivo* of the Trp Triad Mutants

Previous studies have indicated that in *cry2*, the flavin in the dark is in the oxidized (bright yellow) redox state, whereas it becomes

reduced subsequent to light activation and formation of the neutral radical (pale yellow) (Banerjee et al., 2007). This flavin absorption change upon illumination is in fact visible to the naked eye in concentrated protein samples. In whole Sf21 cell cultures (a continuous cell line developed from the moth *Spodoptera frugiperda*), it was found by visual inspection that pellets from cultures expressing high levels of wild-type and mutant cry2 proteins were yellow compared with uninfected control cell cultures (Figure 1), consistent with flavin bound to cry2 in the fully oxidized state. Interestingly, when cells expressing Trp triad mutant receptors were irradiated with white light, a visible color change could be observed in the cells (Figure 1), suggesting redox transition from oxidized to more reduced forms of flavin.

Next, we directly characterized the redox forms of flavin generated in living cells expressing the cry2 mutant proteins. As shown in previous reports, it is possible to detect flavin radical formation after illumination of intact living insect cells expressing cryptochromes from various sources by EPR analysis of whole cell samples (Banerjee et al., 2007; Bouly et al., 2007). Living Sf21 cells expressing wild-type cry2 and W321A, W321F, W374A, W374F, W397A, and W397F cry2 mutant proteins were illuminated with blue light, then frozen and subjected to EPR analysis for detection of radical formation in response to light (see Methods). In wild-type cry2, significant levels of signal above background were detected, indicating radical formation in the cryptochrome photoreceptors (Figure 2A). Interestingly, most of the mutants (W321A, W374A, W397A, W321F, and W374F) also showed clear signal above that of untransfected control cells, indicating the formation of flavin radical even in the absence of a functional Trp triad (Figures 2B and 2F). The only cry2 mutant, which failed to show a signal-above-noise level, was W397F (Figure 2G). However, the tryptophan-to-alanine mutants in particular conclusively show that amino acid substitutions of the Trp triad retain photochemical activity in vivo.

Photoactivation and Flavin Radical Formation of the Trp Triad Mutants in Whole-Cell Lysates

The seeming paradox that in vivo photoreduction occurs in Trp triad mutants whereas they do not undergo photoreduction in vitro had already been noted in earlier studies (Hoang et al., 2008). In order to address this puzzle, we first determined whether photoreduction of cry2 Trp triad mutant proteins could

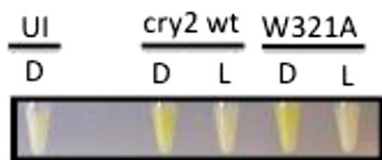


Figure 1. Flavin Reduction of cry2 Trp Substitution Mutant in Insect Cell Expression Culture.

Cells at equivalent cell density expressing wild-type cry2 protein (cry2 wt), the Trp triad mutant (W321A), or uninfected control cell cultures (UI) were resuspended in PBS and photographed either before (D) or after 30 min illumination in white light (L) on ice. Yellow color is from oxidized flavin of expressed protein.

be observed in whole-cell lysates using optical (UV/Vis) spectroscopy. Cell cultures expressing cry2 proteins were lysed in PBS buffer, centrifuged to remove particulate matter, and illuminated for three minutes by blue light in the absence of exogenous reducing agents. Under these conditions, photochemical transformation of expressed cry2 can be clearly resolved in light minus dark difference spectra (Figure 3A). In cell extracts from cultures expressing wild-type cry2 proteins, photoreduction and flavin radical formation is followed by slow reoxidation after return to darkness (Figure 3A, right panel); this difference spectrum appears identical to the photoreduction/reoxidation spectrum for isolated cry2 protein (Banerjee et al., 2007). Illumination of untransformed control cell lysates under the same conditions resulted in no absorbance changes (Figure 3A, left panel), indicating the signal was not due to endogenous flavoproteins in the cultures. It is significant that robust photoreduction occurred even in the absence of added reductants (such as β -mercaptoethanol), suggesting that endogenous reductants were present in the cellular extracts. Thus, the complete photocycle (photoreduction to the flavin radical state by light followed by reoxidation to the flavin oxidized state in the dark) of cry2 proteins could be visualized in crude cell extracts.

To test whether Trp triad mutants were photochemically active in cell lysates, crude lysates were prepared of insect cell cultures expressing the cry2 mutants W321A, W374A, and W397A, as indicated in Figure 3B. These mutants had been previously reported to be photochemically inactive in vitro (Li et al., 2011) but showed a radical signal in vivo (Figure 2). Again, cell lysates from mutant cell cultures were subjected to illumination and difference spectra (light minus dark) were obtained to determine photochemical activity (Figure 3B). Indeed, we observed that all of these mutants showed clear evidence of flavin reduction, even in the complete absence of external reductants (Figure 3B, solid trace). These results are consistent with observed radical accumulation in living cells (Figure 2) and with the reported light-dependent biological activity of these mutants in the cry2 proteolysis assay (Li et al., 2011).

Low Molecular Weight Soluble Factors Enhance Photoreduction in Cell Extracts

To address the question of what cellular components may facilitate photoreduction of Trp triad mutants in vivo, simple fractionation was performed by dialysis of crude lysates through tubing with a molecular weight cutoff of 3500 kD. This tubing retains most proteins and higher molecular weight components but lower molecular weight components are removed. Cell lysates were accordingly subjected to photoreduction both before and after dialysis, without addition of exogenously added reductant.

In the case of wild-type cry2 protein, photoreduction activity was virtually identical both before and after dialysis (Figure 3B, upper left panel). This indicates that in these cellular extracts photoreduction of wild-type cry2 proteins (Banerjee et al., 2007; Li et al., 2011) occurred in the absence of small soluble cellular agents. By contrast, the three Trp substitution mutants W321A, W374A, and W397A showed virtually no photoreduction activity after dialysis, under the same illumination conditions at which

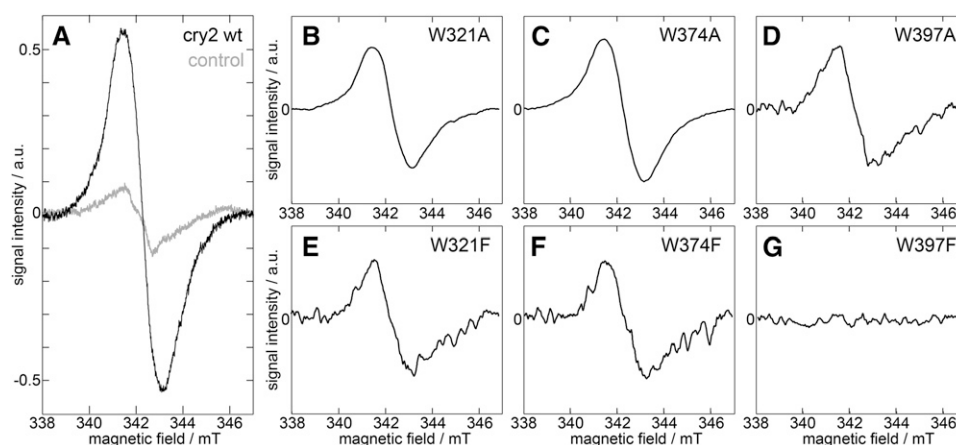


Figure 2. cw-EPR Spectra of Cells with cry2 Wild Type and Mutants after Illumination at 450 nm.

(A) Example of an uncorrected wild-type cry2 spectrum (black) and a control uninfected cell sample (gray).

(B) to (G) Spectra from samples expressing the indicated mutant receptors after subtraction of control and smoothing. All mutants except for W397F show a flavin radical signal above background levels.

they had been activated in the whole-cell lysates (Figure 3B, dotted line) and in which wild type cry2 proteins are reduced (Figure 3B). This result indicates that certain soluble, small molecules removed by the dialysis promote photoreduction of these mutants *in vivo*.

A directed approach was taken to identify possible facilitator molecules, proceeding from the observation that cry has affinity for nucleotide based cofactors such as ATP (Bouly et al., 2003; Brautigam et al., 2004). We reasoned that small molecules that facilitate flavin reduction in lysates must have affinity for the cry2 protein, since lysis of the culture introduces a dilution factor of ~5-fold (see Methods). We accordingly tested the ability of added ATP as well as of the nucleotide based cofactors NADH and NADPH to restore photoreduction activity to dialyzed extracts of the W374A protein. This mutant, shown to be photochemically inactive as an isolated protein (Li et al., 2011), retained the most *in vivo* light-dependent biological activity in a previously performed cry2 degradation assay in living plants (Li et al., 2011) but was not photochemically active in dialyzed samples (Figure 3B). In all cases, addition of 1 mM ATP, 1 mM NADH, and 1 mM NADPH enhanced the photoreduction activity of the W374A mutant in dialyzed protein extracts (Supplemental Figure 1). We accordingly tested these agents on isolated proteins.

Low Molecular Weight Soluble Factors Enhance Photoreduction in Isolated Proteins

From the results with crude extracts, it is not clear whether small metabolites may act as cofactors modulating the activity of other proteins in the extracts that in turn promote cry reduction or whether they interact directly with the cryptochrome itself. We therefore focused on the effects of small metabolites on photoreduction of the purified W374A mutant proteins *in vitro* (Figure 4). Consistent with prior reports, very little photoreduction activity was observed in this mutant, even in the presence of abundant exogenous reductant (10 mM β -mercaptoethanol)

(Figure 4B). However, addition of cofactors (1 mM ATP, NADH, or both) visibly enhanced photoreduction. These effects were apparent already at concentrations in the micromolar range for ATP and NADH (Supplemental Figure 2) and, therefore, well within the physiological range of these compounds in most organisms (Blatt, 1987; Albe et al., 1990; Bennett et al., 2009). To more precisely determine the affinity of cry for ATP, we directly obtained a binding constant (K_D) for cry2 of 49 μ M (Supplemental Figure 3). As a control, we determined the binding constant of ATP for cry1 of 23 μ M under the same experimental conditions, which was in good agreement with the published value of 19.8 μ M (Bouly et al., 2003). At cellular ATP concentrations reportedly in the millimolar range (Blatt, 1987), it follows from these values that both cry1 and cry2 should be fully ligand bound. In summary, cofactors at the physiological concentrations found in living cells should enhance the light sensitivity of plant cryptochromes.

A possible mechanism whereby the cellular metabolites may promote photoreduction in cryptochromes is to serve either directly as electron donors like DTT or indirectly by stimulating electron transfer within the cry2 holoprotein. Even though an action of ATP as reducing agent is unlikely, photoreduction of the W374A mutant was performed in the presence of 1 mM inosine triphosphate (ITP; the oxidized form of ATP) as well as of ADP and AMP. Photoreduction activity was enhanced in all cases (Figures 4B and 4C), indicating that a direct role for ATP as reducing agent can be ruled out as expected.

NADH and NADPH could conceivably play a direct role as endogenous cellular reducing agents, as found in the case of isolated *Escherichia coli* photolyase, a member of the cryptochrome/photolyase gene family, which is normally fully reduced *in vivo* (Supplemental Figure 4). Although not as effective as DTT in causing a significant fraction of photolyase to be reduced, addition of 1 mM NADH, NADPH, and glutathione were able to function as efficient substrates for photoreduction of this photolyase (similar half-lives of oxidized FAD for all tested

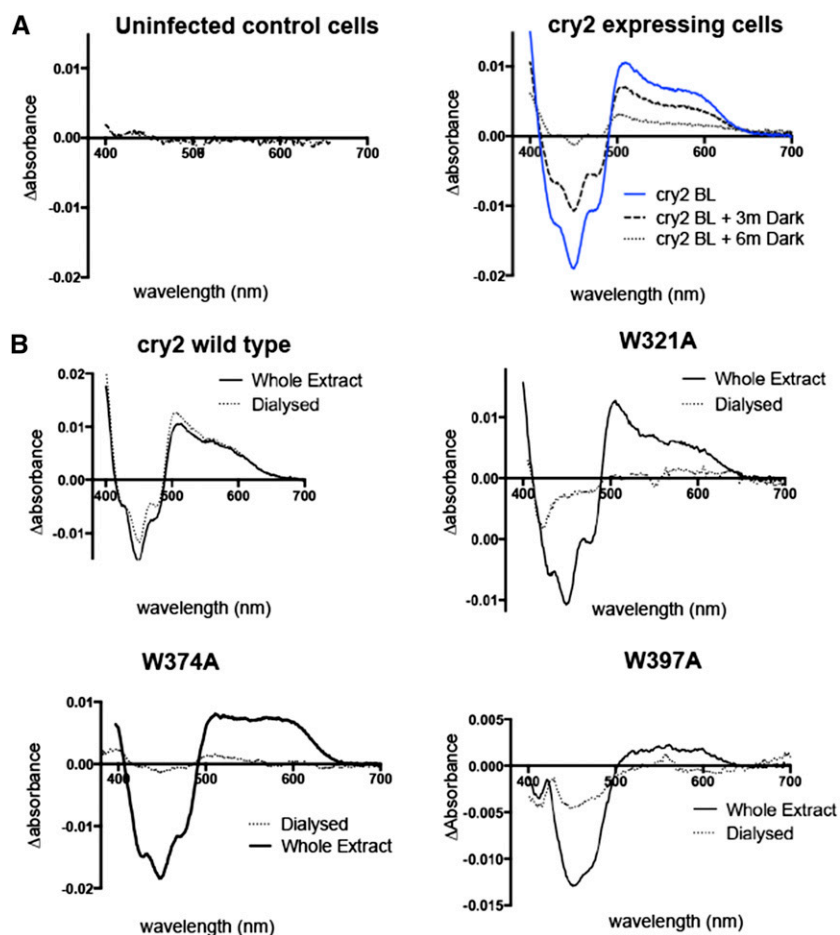


Figure 3. Flavin Photoreduction of *cry2* Wild-Type and Trp Triad Substitution Mutants in Insect Cell Culture Lysates.

(A) Difference spectra of uninfected control whole cell lysates of insect cultures (left panel) and of *cry2* expressing insect cells (right panel) after blue light illumination. Light minus dark difference spectra are shown. Spectra were taken immediately after irradiation and in the course of subsequent reoxidation after return to darkness for 3 and 6 min for *cry2* (right panel). Blue light intensity was $60 \mu\text{mol m}^{-2} \text{s}^{-1}$.

(B) Difference spectra (light minus dark) of wild type and *cry2* mutants subsequent to blue light illumination. Whole-cell extracts were divided into two identical halves and one half subject to dialysis whereas the other was kept on ice. Solid lines, spectra of whole cell extracts; dotted lines, spectra taken under the same illumination conditions of dialyzed samples. Blue light intensity was $60 \mu\text{mol m}^{-2} \text{s}^{-1}$.

[See online article for color version of this figure.]

reductants). However, in the case of cryptochrome, NAD^+ was equally effective as NADH in promoting photoreduction in isolated proteins (Supplemental Figure 5), indicating that NAD(H)-driven photoreduction occurs independent of the redox state. A minor role as reducing agent is not excluded by the data and may explain additive effects of adding several metabolites in saturating concentrations in cellular extracts (Supplemental Figure 1).

As an alternate mechanism, metabolite binding to a site within the protein may induce a conformational change that affects subsequent response to illumination. This possibility is consistent with prior reports showing that ATP binding indeed induces conformational change in *Arabidopsis cry1* even in the absence of illumination (Burney et al., 2009). To verify whether this mechanism may also occur for *cry2*, we performed partial tryptic proteolysis with isolated *cry2* in the presence and absence of

ATP (Supplemental Figure 7). The obtained differential proteolytic patterns indicate a conformational change caused by nucleotide binding and suggest a change in rigidity of *cry2*, when exposed to in vivo-like conditions.

ATP Enhances Effectiveness of Electron Transfer in *Arabidopsis cry2*

The remaining question is therefore by what means these small metabolites enhance the photosensitivity of cryptochrome. One possibility may be that ATP and related metabolites can stabilize the radical form of the isolated *cry* protein that is formed subsequent to illumination, as previously shown to occur in vitro in algal *cry1* (Immeln et al., 2007). This would result in significantly reduced rates of flavin reoxidation in the presence of added ATP

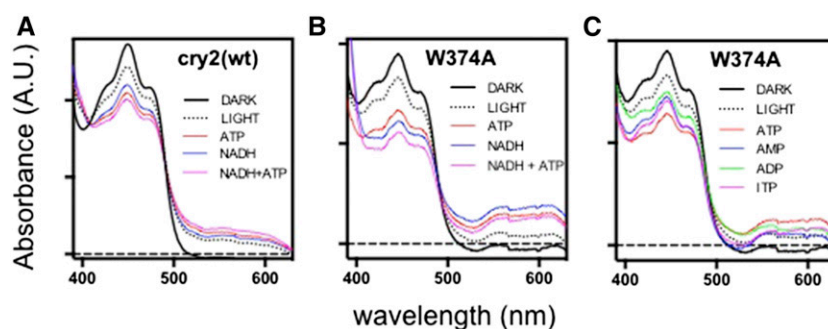


Figure 4. Effect of Small Metabolites on Flavin Photoreduction in Purified cry2 Wild-Type and W374A Mutant Proteins.

Isolated proteins were illuminated in white light (WL; $400 \mu\text{mol m}^{-2} \text{s}^{-1}$) in the presence of 10 mM β -mercaptoethanol prior to obtaining spectra. Dark: unilluminated samples.

(A) Illumination of $100 \mu\text{M}$ wild-type cry2 for 10 s in the absence (LIGHT) or presence of 1 mM ATP, 1 mM NADH, or 1 mM of each ATP and NADH.

(B) Illumination of $50 \mu\text{M}$ W374A for 180 s in the presence of ATP, NADH, or both metabolites.

(C) Illumination of $50 \mu\text{M}$ W374A in the presence of 1 mM ATP, AMP, ADP, or ITP.

and, thus, an increased signal in Trp triad mutants (Figures 1 to 3) in whole cells when radicals accumulate due to their increased stability. Alternatively, the primary electron transfer reactions themselves may be rendered more efficient in an *in vivo* context.

To help resolve this question, EPR spectroscopic measurements were made on isolated cry2 wild-type and mutant proteins. First, *cw*-EPR (continuous-wave EPR) measurements at cryogenic temperatures were performed to determine flavin radical accumulation subsequent to illumination of isolated proteins. These measurements revealed a significant increase in flavin radical concentration in the presence of added ATP for both wild-type cry2 protein samples, as well as the Trp triad mutant W374A (Figures 5A and 5B). These results are consistent with the results of optical studies from isolated proteins (Figure 4).

To determine whether the actual forward electron transfer can be altered by the presence of ATP, transient EPR experiments were performed on cry2 wild type as well as W374A and W321A mutants. The wild-type spectra in the absence of ATP (Figure 6B, dashed) show an emissive-adsorptive pair of lines split by $\sim 15\text{G}$. This feature arises due to a radical pair (RP) forming between the flavin and a distal Trp or Tyr radical (Biskup et al., 2011) and is a direct indicator for the forward electron transfer reaction. In W321A, with its interrupted Trp triad, the distal RP signal is still discernable (Figure 6D, dashed), indicating that there are other electron transfer pathways available, as has been reported previously (Biskup et al., 2011, 2013), albeit with a significantly reduced quantum yield. In W374A (Figure 6C), this signal has dropped below the detection level of our experiment.

However, upon addition of ATP, a significant enhancement in RP signal is observed. Comparing the ATP-less (Figure 6, dashed line) spectra of the various proteins with their counterparts after the addition of 10 mM ATP (Figure 6, solid lines) shows that ATP increases the amplitude of the signal. Since these changes in signal intensity are for the most part large and also not accompanied by significant changes in spectral width and shapes (which would indicate a shift in magnetic parameters of the sample), they indicate that ATP addition significantly

increases the quantum yield of the electron transfer reaction in the wild type as well as in the mutant (Biskup et al., 2013). This effect is strongest in the Trp triad mutants W374A and W321A (Figures 6C and 6D, solid), which by definition indicates that alternate electron transfer pathways distinct from the Trp triad are being potentiated by ATP. The effect is less pronounced in the wild-type cry2 protein (Figure 6B), likely because electron transfer through Trp triad is already quite efficient at 274K and at the light intensity used for these experiments. Nonetheless, even

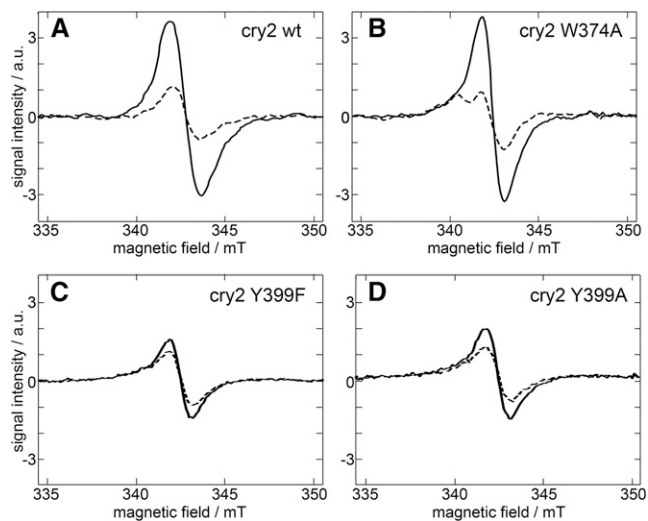


Figure 5. *cw*-EPR Spectra of Isolated Proteins after Illumination at 450 nm.

cw-EPR spectra of flavin radical accumulated in cry2 wild type **(A)** and W374A, W399F, and W399A mutant **(B)** to **(D)** proteins in the presence (solid) and absence (dashed) of 10 mM ATP. Spectra were normalized to the signal intensity in the absence of ATP for all samples. cry2 wild type as well as the W374 mutant of cry2 show a distinct and similar increase of flavin radical signal in the presence of ATP, while the effect for both the Y399F and the Y399A cry2 variants are strongly reduced.

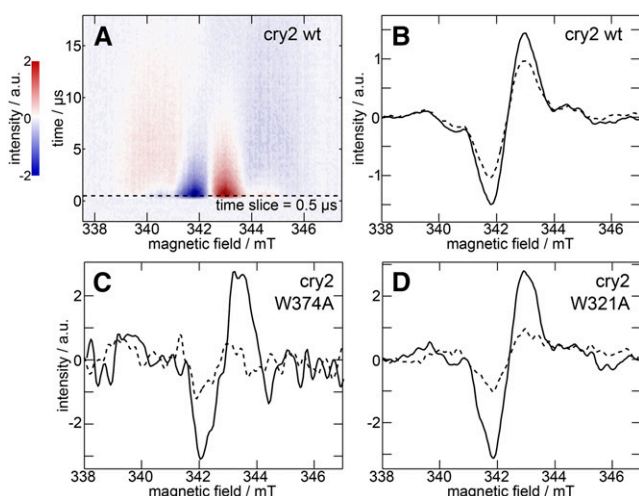


Figure 6. Transient EPR Spectra of Isolated Proteins at 274K after 450-nm Laser Excitation.

(A) Example 2D data set of cry2 wild type.

(B) to (D) Slices along the magnetic field at $t = 0.5 \mu\text{s}$ from spectra of cry2 wild type as well as cry2 mutant proteins W374A and W321A, all in the presence (solid) and absence (dashed) of 10 mM ATP. All three samples show a distinct increase in signal intensity in the presence of ATP, with the two mutant proteins exhibiting a much larger effect than the wild type.

in wild-type protein, there is measureable and reproducible effect of ATP on electron transfer. This dependence of the RP yield on the presence of ATP in cry2 is in agreement with observations from isolated wild-type cry1 (Müller et al., 2014).

Alternate Electron Transfer Pathways Are Implicated in ATP-Sensitive Flavin Reduction in cry2 Protein

The data presented above show that ATP enhances RP yield and, thereby, electron transfer in Trp triad mutants. Such alternate electron transfer pathways that may mediate photoreduction in the absence of W374 of the Trp triad in cry2 can be immediately suggested on the basis of the *Arabidopsis* cry1 structure. These include redox-active W376 and W331, at distances of 9.5 and 13.5 Å from the surface-exposed, distal W321 and 10.7 and 7.7 Å from the flavin-proximal W397, respectively. As a second possibility, the structure of *Arabidopsis* cry1 with added ATP shows that the adenine moiety is located only 11 Å away from the isoalloxazine ring of the FAD chromophore and thereby suitably positioned to form an alternative electron transfer pathway to redox-active surface residues such as Y402 (cry2: Y399). Therefore, Y399 in combination with ATP or other metabolites binding may provide an electron transfer pathway independent of, and additive to, the classic Trp triad pathway.

To test these possibilities, the following amino acid substitutions were made in the *CRY2* gene and the expressed isolated proteins tested for photoreduction: W331A, W374F, W376A, Y399A, and Y399F (Figure 7). The isolated proteins were illuminated in vitro in the presence or absence of added ATP to determine whether flavin radical formation is enhanced.

Interestingly, mutations W331A and W376A showed decreased light sensitivity compared with wild-type protein even in the absence of added metabolite, since illumination times of 120 s were required to obtain photoreduction comparable to wild-type protein (cry2) achieved after only 10 s of illumination. Furthermore, W374F showed apparent greater light sensitivity than the W374A mutant under the same illumination conditions. These results suggest that even in the wild-type protein, there are branch points in the classic Trp triad electron transfer chain involving W376 and W331 redox active amino acids (Figure 7, W331A and W376A compared with W374A; Figure 4). Importantly, all of these mutants showed significantly enhanced photoreduction in the presence of added ATP. This indicates either that there is redundancy in electron transfer pathways potentiated by ATP or that there are other unrelated ATP sensitive electron transfer pathways.

In this context, interesting observations resulted from analysis of the Y399A and Y399F amino acid substitutions. Both the Y399A and Y399F mutants could be efficiently photoreduced in vitro under the same illumination conditions as wild-type proteins; however, their response to added 1 mM ATP was significantly decreased compared with the wild type under the same illumination conditions (Figures 7E and 7F). This effect was surprising as it could indicate an additional mechanism of electron transfer for cryptochromes. We therefore performed an additional verification of this result by EPR measurements on isolated Y399A and Y399F protein samples (Figures 5C and 5D). In both cases, signal amplification as a result of added metabolites was significantly reduced compared with wild-type protein or other mutants illuminated under the same redox conditions (Figures 5A and 5B). We further verified that ATP binding affinity for the Y399 mutant proteins remained intact. We first determined that isolated Y399A mutant protein has a K_d for ATP binding of 15 μM , which is on the order of magnitude and even somewhat lower than for cry2 (Supplemental Figure 3A). We further demonstrate that both Y399F and Y399A mutant proteins are bound to ATP agarose columns and eluted specifically at 1 mM ATP concentration (Supplemental Figure 3C). Decreased sensitivity to ATP in these mutants is therefore consistent with an alternate electron transfer pathway through adenine from flavin to the surface-exposed Y399 residue.

DISCUSSION

The principal motivation behind this work has been to find the origin of seemingly contradicting results on the role of the Trp triad in cryptochrome flavin photoreduction and light signaling. Over the past few years, several studies have proceeded from the identical assumption that in vitro observations of flavin reduction in isolated proteins correspond to the physical state of the receptor in vivo to reach conclusions concerning the role of flavin redox state transition and biological activity. We demonstrate with the data presented here that *Arabidopsis* cry2 in fact behaves very differently in an in vivo context than it does as an isolated protein. Even to the naked eye (Figure 1) it is apparent that Trp triad mutants, which reportedly undergo no photoreduction in vitro (Li et al., 2011), are photochemically active in vivo. Further experiments using EPR spectroscopy demonstrate

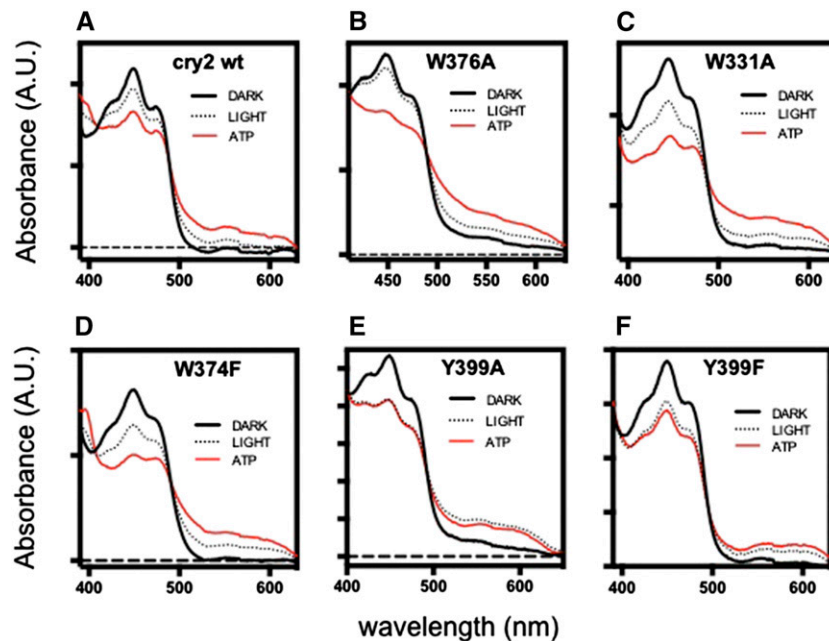


Figure 7. Responsivity of Wild-Type and Mutant cry2 Proteins to White Light in the Presence or Absence of Added ATP.

Purified proteins of the indicated mutants were photoreduced in PBS buffer in the presence or absence of 1 mM added ATP.

(A), (E), and (F) Samples were irradiated for 10 s at $400 \mu\text{mol m}^{-2} \text{s}^{-1}$.

(B) to (D) Samples were irradiated for 120 s at $400 \mu\text{mol m}^{-2} \text{s}^{-1}$.

that the Trp substitution mutants W321A, W321F, W374A, W374F, and W397A of *Arabidopsis* cry2 clearly undergo light-dependent radical formation in vivo (Figure 2). Finally, UV/Vis spectroscopy directly detects forward (flavin reduction) and reverse (flavin reoxidation) redox state transitions of Trp triad mutant proteins within whole-cell extracts (Figure 3). These results show that Trp triad mutants of cryptochromes are photochemically active and undergo photoreduction in a cellular context. Therefore, conclusions regarding in vivo photochemical redox state transitions cannot be drawn from analysis of Trp triad mutants in vitro for plant and likely also insect cryptochromes (Song et al., 2007; Oztürk et al., 2008; Li et al., 2011; Oztürk et al., 2011, 2013, 2014).

An additional interesting outcome of this study has been the characterization of an unusual mechanism of signaling modulation by cryptochromes. We determined that at least part of the difference between in vitro and in vivo photochemical activity of cry2 can be attributed to the presence of small metabolites such as ATP that increase the yield of the distal RP formed by electron transfer, including in the cry2 W374A mutant. This work therefore shows that in vivo photoreduction occurs by the classic Trp triad route as well as alternative routes that are not efficiently used in isolated proteins. The concentrations of cofactor required for these effects (Supplemental Figures 2 and 3) are well within the physiological range of millimolar concentration of ATP reported in the plant cytosol (Blatt, 1987). Additional metabolites containing an adenine moiety [for instance, ADP and NAD(P)H] are also effective in potentiating cryptochrome photoreduction (Figure 4).

The mechanism whereby these metabolites exert their role on photoreduction is unlikely to be by acting as cellular reducing agents. Both ATP and its oxidized form ITP are effective in promoting photoreduction, excluding a primary role as electron donor. Although NADH and NADPH are somewhat effective in vitro as reducing agents for *E. coli* photolyase (Supplemental Figure 4), NAD^+ is effective as well as NADH in promoting cry2 W374A photoreduction (Supplemental Figure 5) and thereby also excluding a primary role as reductant. Our results suggest instead that all of these cofactors may in fact function by a similar mechanism involving binding to a common site in the cryptochrome. In keeping with this suggestion, it has been possible to elute cryptochrome bound to an ATP agarose affinity column by addition of NADH, which is consistent with a common binding site and similar mechanism of activation (Supplemental Figure 6). Nevertheless, given some indication of additive effects of NADH with ATP (Figure 4; Supplemental Figure 1), an additional secondary role for NADH and/or NADPH as cellular reducing agent cannot be excluded.

The most probable mechanism consistent with our results is that metabolite binding causes small structural and/or charge distribution changes to facilitate alternative electron transfer pathways. For example, the crystal structure of *Arabidopsis* cry1 with ATP shows that the adenine moiety is only 11 Å distant from the isoalloxazine ring of the FAD chromophore and thereby suitably positioned to form an alternative electron transfer pathway to redox-active surface residues such as Y402 (cry2: Y399). Consistent with this suggestion, we show that mutations at this position (Y399A and Y399F) show significant decrease in

responsivity to ATP (Figures 6 and 7). Although we cannot exclude alternate explanations such as small structural perturbations in the flavin binding pocket resulting from the Tyr substitution, this seems unlikely. The Y399F mutation is conservative, flavin binding and photoreduction appear unaffected (Figure 7), and ATP is efficiently bound (Supplemental Figure 3) for both Y399A and Y399F. It is therefore possible that electron transfer between the phenolic group of Y399 and the isoalloxazine may be fostered by tunneling events through the adenine moieties of ATP and the FAD cofactor or due to the changed dielectric constant within the pathway. The latter is a crucial parameter in the Marcus' theory of electron transfer, as it describes the polarization features of the reaction coordinate and hence affects the achievable rates for charge separation. In either event, a Y399-ATP-FAD route would represent a pathway that contributes to enhanced photoreduction even in wild-type proteins (Figure 8). As a precedent for such a mechanism, the role of nucleobases has been extensively discussed in the context of long-range electron transfer in DNA (Giese, 2002; Muren et al., 2012).

Additional means whereby electron transfer pathways could be potentiated by metabolite binding must also exist, given residual ATP dependent response in the Y399A and Y399F mutants (Figures 5 and 7). We have accordingly examined mutations of W376 and W331 residues, which are not part of the classic Trp triad and are located at distances of 9.5 and 13.5 Å from the surface-exposed, distal W321 and 10.7 and 7.7 Å from the flavin-proximal W397, respectively (Figure 7). In the case of both W331A and W376A mutants, there is a decline in photosensitivity, suggesting that these alternate routes are to some degree used even in wild-type proteins, together with W374. One suggestion on how metabolite binding may modulate electron transfer from these existing pathways follows from the demonstration that ATP binding induces structural changes independently of light in both *Arabidopsis* cry1 (Burney et al., 2009) and cry2 (Supplemental Figure 7). Altered accessibility of the protein surface to added protease can result from increased flexibility in the cry apoprotein (Fontana et al., 2004; Partch et al., 2005). Although these changes do not by themselves activate

cry in the dark, a consequence of altered protein flexibility could be improved alignment of alternate electron transfer residues W331A and W376A with the flavin-proximal W397 and flavin-distal W321, resulting in more efficient electron transfer subsequent to illumination. A contribution of ATP toward potentiating these alternate (W331A and W376A) pathways is therefore consistent with our findings (Figure 8). As a precedent for such a mechanism, in the much more complex nitrogenases, ATP binding is required to promote electron transfer to N_2 (Duval et al., 2013). Similarly, ATP binding is required to drive electron transfer to B_{12} -dependent methyl transferases for their activation (Hennig et al., 2014).

Possible mechanisms to be derived from the literature include a suggestion that ATP binding may enhance photoreduction efficiency by raising the pK_a of D396 (D393 in cry2), a residue that donates a proton to nearby flavin subsequent to electron transfer (Cailliez et al., 2014; Müller et al., 2014). This suggestion is not incompatible with our findings, since data on increased amplitude of RP formation in truncated cry1 (Müller et al., 2014) agree with our observations for cry2. However, we find that added ATP enhances cry2 photoreduction even at pH 5.7 (Supplemental Figure 8), where D393 in cry2 is likely fully protonated (Brautigam et al., 2004) and therefore should not be affected by an increase in pK_a resulting from metabolite binding. The claim that ATP effects on a truncated fragment of cry1 occur already at pH 6.5, where D396 should be fully protonated (reported $pK_a = 7.4$) (Müller et al., 2014), is also in seeming contradiction to this model. An alternative relevant observation is that ATP binding significantly increases the stability of the flavin neutral radical in an algal cry1 homolog and thereby its accumulation subsequent to illumination (Immeln et al., 2007, 2010). This effect is also compatible with our data as we see significantly higher radical accumulation in the presence of ATP in vivo. However, this mechanism cannot explain the increase in RP signal (Figure 6) as flavin neutral radical formation occurs only subsequent to electron transfer. Therefore, although we cannot exclude some contribution through this means (Immeln et al., 2007), a mechanism whereby electron transfer is

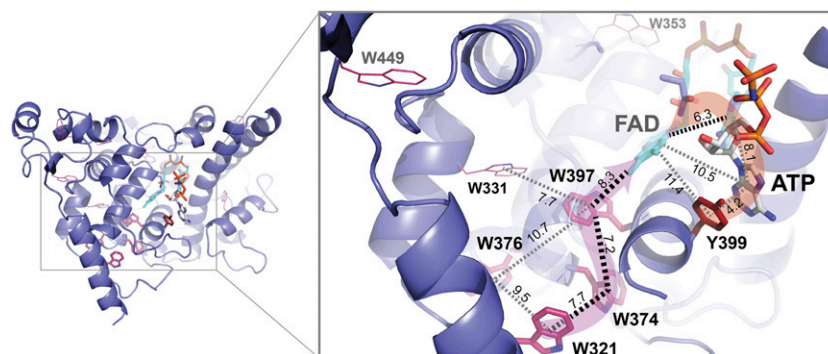


Figure 8. Electron Transfer Pathways in *Arabidopsis* cry2.

The Cry2 structure was generated by homology modeling using as template the structure of the At-Cry1 adenosine-5'-(β , γ -imido)triphosphate (AMPPNP) complex (1U3D, sequence identity 60%; Brautigam et al., 2004) and the program suite MODELER v9.11 (Sali and Blundell, 1993). Distances between aromatic moieties are given in Angstrom and depicted as dashed lines. The electron transfer pathway of the classical Trp triad, FAD-W397-W374-W321, is highlighted by a purple arrow. Alternative pathways may be formed from Y399 via ATP (orange arrow) or by aromatic residues near the Trp triad (W331 and W376). Compared with Cry1, the ATP binding site of Cry2 is highly conserved apart from N356 (Cry1: D359) and R289 (Cry1: K292).

potentiated via electron tunneling through ATP and Y399, as well as through greater transient alignment of multiple alternative branches within the Trp triad pathways, seems a more likely explanation for our *in vivo* observations. The position of the amino acid residues with respect to flavin and ATP binding sites and the delineation of the alternate electron transfer pathways suggested by this study are shown in the context of the modeled cry2 protein structure (Figure 8).

In summary, we demonstrated that *in vivo* properties of flavoproteins can differ markedly from those observable *in vitro*, even with respect to their primary photochemistry. Our observations shed light on a long-standing debate concerning the role of flavin reduction and the Trp triad in cry biological function and moreover identified a potential new route for electron transfer that is independent of the Trp triad. Our results do not exclude additional mechanisms and means by which the intracellular environment may tune flavin photochemistry, for instance, the identity and role of the intracellular reducing agent remains to be conclusively demonstrated. This work should therefore help to stimulate future research into many new areas as it becomes increasingly evident that cry photochemistry can be fully grasped only in the context of the intracellular environment.

As a final point of interest, emerging evidence suggests that the feature of cry activation by metabolites may be of general relevance. For example, Trp triad mutants of *Drosophila* cryptochrome (Dm-Cry) also fail to undergo photoreduction *in vitro* but retain biological signaling function (Song et al., 2007; Oztürk et al., 2008) and undergo photoreduction *in vivo* (Hoang et al., 2008; Gegear et al., 2010; Vaidya et al., 2013). This is consistent with some form of *in vivo* modulation of light sensitivity in *Drosophila* cryptochrome. The situation becomes even more interesting in the case of mammalian cryptochromes, which function in the absence of light. Here, metabolite binding might induce structural changes that directly affect interaction with signaling partners independently of light. In line with such a conclusion is the *cop*-like phenotype of the cry1 L407F mutant, which mimics an activated conformation independent of light exposure (Exner et al., 2010). Likewise consistent with this view is evidence of ATP binding to human Cry1 (Bouly et al., 2003). In addition, the mammalian circadian clock has been strongly linked to cellular metabolic state (Asher and Schibler, 2011), raising the possibility of modulation of cry activity by cellular metabolite concentration. Further recent observations have shown that biological activity of mammalian cryptochromes in the circadian clock can be directly altered by interaction with small synthetic compounds (Hirota et al., 2012), which may mimic other natural, as yet unknown metabolites. Therefore, cry activity *in vivo* may well be regulated by multiple physiological modulators, which could provide the basis for unprecedented pharmacological interventions in the future.

METHODS

Mutant Construction and Protein Expression

Site-directed mutagenesis of tryptophans of the Trp triad in *Arabidopsis thaliana* cry2 was performed using the QuikChange site-directed mutagenesis kit (Stratagene) and full-length CRY2 gene cloned into *EcoRI/NotI* sites of vector pET-28a(+) (Novagen) as template. The primer

combinations were as follows (Wor Y codon replaced by A or F codon in small letters): W321A forward 5'-GTTTTTCCCTgcaGATGCTGATGTTGA-3' and reverse 5'-TCAACATCAGCATctgcAGGGAAAAAC-3'; W374A forward 5'-CTTCCATGGAAAgaGGAATGAAGTATT-3' and reverse 5'-AATACTTCATTCCtgctTTCCATGGAAG-3'; W397A forward 5'-GTGACATCCTGGCGcaCAGTATATC-3' and reverse 5'-GATATACTGtgcGCCAAGGATGTCAC-3'; Y399F forward 5'-CATCCTTGGCTGGCAGttTCTCTCTGGGAGTATCC-3' and reverse 5'-GGATACTCCAGAGATaaCTGCCAGCCAAGGATG-3'; Y399A forward 5'-GACATCCTGGCTGGCAGgccATCTCTCTGGGAGTATCCCC-3' and reverse 5'-GGGGATACTCCAGAGATggcCTGCCAGCCAAGGATGTC-3'; W331A forward 5'-GTTGATAAGTTCAAGGCCgccAGACAAGGCAGGACCCGT-3' and reverse 5'-ACCGTCTGCCTTGTCTgcccGGCCTTGAACCTTAAAC-3'; W376A forward 5'-GAAGTTTCTTCTCCTTCCATGAAAagccGGAATGAAGTATTTCTGGGAT-3' and reverse 5'-ATCCCAGAAATACTTCATTC-CggcTTTCCATGGAAGGAGAAGAACTTC-3'. cry2 amino acid substitution mutants were made by the primer combinations as described (Li et al., 2011). The correctness of the resulting products was verified by sequencing. The inserts were released by digestion with *XbaI* and *NotI*, yielding an N-terminal 6xHis-tag, and inserted into the *XbaI* and *NotI* sites of vector pBacPAK9 (Clontech). These plasmids were cotransfected with linearized BacPAK6 viral DNA into Sf21 insect cells (Clontech).

EPR Spectroscopy

To ensure homogenous illumination of the sample, the EPR tubes were mounted centrally in a reflective cylinder with 40-mm inner diameter and illuminated from opposite sides using dual 5-mm optical fibers from Stoppel. Total irradiance at the sample position was 6.8 ± 0.2 mW/cm² at 450 nm at the sample position. For cell samples, multiple samples illuminated for 10, 20, and 30 min were investigated to verify that saturation of the turn over into the light-induced state was achieved. For purified protein, two samples for each variant were prepared, both with the same amount of sample, but one with 10 mM ATP added. Samples were illuminated for 10 min with the setup described above and then rapidly frozen.

Purified protein intended for transient EPR had 10% glycerol to ensure a liquid sample at 274K and 5 mM K₃Fe(CN)₆ to enable flavin reoxidation added. Two samples each, with and without 10 mM ATP, were produced from the same stock, with the ATP-less sample topped up with water to ensure identical protein concentrations. Samples were then transferred into 1.0/2.0-mm inner/outer diameter quartz sample tubes and kept at 2°C until transferred to the spectrometer.

Both *cw*-EPR and transient EPR experiments were performed on lab-built X-Band spectrometers. The spectrometer used for *cw*-EPR consists of a microwave bridge ER 041 MR, microwave controller ER 048 R, magnet power supply ER 081 S, and field controller BH 15, all from Bruker. The resonator used was a Bruker ER 4122 SHQ E cavity resonator; for signal detection, a Stanford Research SR810 lock-in detector was used. Microwave frequency measurements were performed using an Agilent 53181A frequency counter.

Transient EPR experiments were performed using an ER 046 XK-T microwave bridge, ER 048 R microwave controller, and a BH 15 field controller, all from Bruker, as well as a Varian V7900 magnet power supply. An ER 4118X-MD5 resonator was used.

The sample was excited using a SpectraPhysics DCR-11 Nd:YAG laser with an OPTA OPO at 450 nm. The EPR signal was detected using a LeCroy WaveRunner 104MXi as a transient recorder. The microwave frequency was measured using a Hewlett Packard 5352B frequency counter.

For *cw*-EPR, the samples were measured with 2-G modulation amplitude, 100-kHz modulation frequency, and 100-ms lock-in time constant. The microwave power was 200 μW and the frequency around 9.38 GHz. For each measurement, the current microwave frequency was

recorded. The spectra are averages over 30 scans. Cell spectra were smoothed using a window of 3% of data points.

For transient EPR, the samples were measured at microwave frequencies of around 9.69 GHz and 2-mW microwave power. cry2 wild-type samples were measured with 1-mJ pulse energy, while W374A and W321A were measured with 1.5 mJ. Each pair (\pm ATP) of samples was measured consecutively to minimize laser power drift, and the pulse energy was constantly monitored. Pulse energy variation over the course of a measurement pair was 10% root-mean-square. The shot repetition rate was 2.5 Hz. Each measurement is the result of 30 scans with 10 shots per point, making for a total of 300 accumulations. Spectra were smoothed using a window of 3% of data points.

cw-EPR measurements were performed at 80K and the transient EPR measurements at 274K. Low temperatures were reached with an Oxford ESR 910 cryostat and Oxford ITC503 temperature controller and a home-built cryostat with LakeShore 321 autotuning temperature controller for cw-EPR and transient experiments, respectively.

Preparation and Analysis of Crude Cell Lysates

Sf21 insect cell cultures expressing recombinant cry2 proteins were harvested 3 d after infection at cell densities at an A_{600} of between 0.6 and 0.8. Cells were pelleted at 1200g for 5 min and gently washed once in PBS (pH 8.0). Pellets were subsequently lysed at 0°C in a 5-fold volume of PBS containing 1% Triton and 1% protease inhibitor cocktail (Sigma-Aldrich). Lysates were pelleted at 14,000g for 60 min at 4°C, and the clarified supernatants recovered for spectrophotometric analysis. Dialysis (where indicated) was performed overnight in PBS buffer using Membra-CEL tubing (MW cutoff 3500; Sigma-Aldrich). Where metabolites were added, samples were allowed to equilibrate for several minutes prior to illumination, and new baseline spectra were taken after each addition to verify that no absorption drift or sample precipitation occurred as a result. Spectra were obtained on a Cary 300 Scan UV/Vis spectrophotometer (Agilent). ATP, ADP, AMP, ITP, NADPH, and NADH were purchased from Sigma-Aldrich.

Cry Protein Purification and Analysis

cry2 wild-type and mutant W374A proteins were isolated from extracts prepared as above using nickel Ni-NTA affinity chromatography as previously described (Banerjee et al., 2007; Bouly et al., 2007). Illumination of isolated proteins was in elution buffer (50 mM phosphate, pH 8.0, 150 mM NaCl, and 250 mM imidazole) and 1% protease inhibitor cocktail (Sigma-Aldrich). Spectra were obtained on a Cary 300 Scan UV/Vis spectrophotometer.

Accession Numbers

Sequence data from this article can be found in the GenBank/EMBL libraries under accession numbers NM_116961 (At-CRY1) and NM_179257 (At-CRY2).

Supplemental Data

The following materials are available in the online version of this article.

Supplemental Figure 1. W374A Mutant Photoreduction in Whole-Cell Lysates after the Addition of NADH, NADPH, and ATP.

Supplemental Figure 2. Photoreduction of Isolated W374A Protein at Different Metabolite Concentrations.

Supplemental Figure 3. ATP Binding Affinity in Wild-Type and Mutant Cryptochromes.

Supplemental Figure 4. Absorbance Changes in *E. coli* DNA Photolyase upon UV Light Illumination in the Presence of Different Reductants.

Supplemental Figure 5. Photoreduction of Isolated W374A Protein in the Presence of NAD and NADP.

Supplemental Figure 6. cry2 Is Eluted from an ATP Agarose Affinity Column by Added NADH.

Supplemental Figure 7. Partial Proteolysis of cry2 in the Presence or Absence of ATP.

Supplemental Figure 8. ATP Binding Facilitates cry2 Photoreduction at Low pH.

Supplemental Methods.

Supplemental References.

ACKNOWLEDGMENTS

We thank Oxana Panajotowa, Jeanette Schermuly, Nils Braun, Jeffrey Steward, and Claire Monné for help with constructions, protein expression, and facilities. We also thank Ringo Wenzel for help establishing EPR measurement protocols and sharing insights on cry1. Funding was from the National Science Foundation (1237986), ANR (ANR-09-BLAN-0248), AFOSR (FA9550-14-1-0409), the Deutsche Forschungsgemeinschaft (Cluster of Excellence EXC-314 'Unifying Concepts in Catalysis,' BI 464/10-1, BA 985/12-1, and BA 985/14-1/SPP 1530), FA9550-14-1-0409, and the Human Frontiers (HFSP-RGP0045).

AUTHOR CONTRIBUTIONS

M.A., A.B., L.-O.E., and R.B. designed research. C.E., X.W., D.R., J.M., and A.B. performed research. M.A., A.B., J.M., and R.B. analyzed data. M.A., L.-O.E., A.B., and R.B. wrote the article.

Received July 23, 2014; revised October 19, 2014; accepted November 4, 2014; published November 26, 2014.

REFERENCES

- Ahmad, M., Grancher, N., Heil, M., Black, R.C., Giovani, B., Galland, P., and Lardemer, D.** (2002). Action spectrum for cryptochrome-dependent hypocotyl growth inhibition in Arabidopsis. *Plant Physiol.* **129**: 774–785.
- Albe, K.R., Butler, M.H., and Wright, B.E.** (1990). Cellular concentrations of enzymes and their substrates. *J. Theor. Biol.* **143**: 163–195.
- Asher, G., and Schibler, U.** (2011). Crosstalk between components of circadian and metabolic cycles in mammals. *Cell Metab.* **13**: 125–137.
- Balland, V., Byrdin, M., Eker, A.P., Ahmad, M., and Brettel, K.** (2009). What makes the difference between a cryptochrome and DNA photolyase? A spectroelectrochemical comparison of the flavin redox transitions. *J. Am. Chem. Soc.* **131**: 426–427.
- Banerjee, R., Schleicher, E., Meier, S., Viana, R.M., Pokorny, R., Ahmad, M., Bittl, R., and Batschauer, A.** (2007). The signaling state of Arabidopsis cryptochrome 2 contains flavin semiquinone. *J. Biol. Chem.* **282**: 14916–14922.
- Bennett, B.D., Kimball, E.H., Gao, M., Osterhout, R., Van Dien, S.J., and Rabinowitz, J.D.** (2009). Absolute metabolite concentrations and implied enzyme active site occupancy in *Escherichia coli*. *Nat. Chem. Biol.* **5**: 593–599.
- Biskup, T., Hitomi, K., Getzoff, E.D., Krapf, S., Koslowski, T., Schleicher, E., and Weber, S.** (2011). Unexpected electron transfer

- in cryptochrome identified by time-resolved EPR spectroscopy. *Angew. Chem. Int. Ed. Engl.* **50**: 12647–12651.
- Biskup, T., Paulus, B., Okafuji, A., Hitomi, K., Getzoff, E.D., Weber, S., and Schleicher, E.** (2013). Variable electron transfer pathways in an amphibian cryptochrome: tryptophan versus tyrosine-based radical pairs. *J. Biol. Chem.* **288**: 9249–9260.
- Blatt, M.R.** (1987). Electrical characteristics of stomatal guard cells: the contribution of ATP-dependent “electrogenic” transport revealed by current-voltage and difference-current-voltage analysis. *J. Membr. Biol.* **98**: 257–274.
- Bouly, J.P., Giovani, B., Djamei, A., Mueller, M., Zeugner, A., Dudkin, E.A., Batschauer, A., and Ahmad, M.** (2003). Novel ATP-binding and autophosphorylation activity associated with Arabidopsis and human cryptochrome-1. *Eur. J. Biochem.* **270**: 2921–2928.
- Bouly, J.P., Schleicher, E., Dionisio-Sese, M., Vandenbussche, F., Van Der Straeten, D., Bakrim, N., Meier, S., Batschauer, A., Galland, P., Bittl, R., and Ahmad, M.** (2007). Cryptochrome blue light photoreceptors are activated through interconversion of flavin redox states. *J. Biol. Chem.* **282**: 9383–9391.
- Brautigam, C.A., Smith, B.S., Ma, Z., Palnitkar, M., Tomchick, D.R., Machius, M., and Deisenhofer, J.** (2004). Structure of the photolyase-like domain of cryptochrome 1 from *Arabidopsis thaliana*. *Proc. Natl. Acad. Sci. USA* **101**: 12142–12147.
- Brettel, K., and Byrdin, M.** (2010). Reaction mechanisms of DNA photolyase. *Curr. Opin. Struct. Biol.* **20**: 693–701.
- Burney, S., Wenzel, R., Kottke, T., Roussel, T., Hoang, N., Bouly, J.P., Bittl, R., Heberle, J., and Ahmad, M.** (2012). Single amino acid substitution reveals latent photolyase activity in Arabidopsis cry1. *Angew. Chem. Int. Ed. Engl.* **51**: 9356–9360.
- Burney, S., Hoang, N., Caruso, M., Dudkin, E.A., Ahmad, M., and Bouly, J.P.** (2009). Conformational change induced by ATP binding correlates with enhanced biological function of *Arabidopsis* cryptochrome. *FEBS Lett.* **583**: 1427–1433.
- Cailliez, F., Müller, P., Gallois, M., and de la Lande, A.** (2014). ATP binding and aspartate protonation enhance photoinduced electron transfer in plant cryptochrome. *J. Am. Chem. Soc.* **136**: 12974–12986.
- Chaves, I., Pokorny, R., Byrdin, M., Hoang, N., Ritz, T., Brettel, K., Essen, L.O., van der Horst, G.T., Batschauer, A., and Ahmad, M.** (2011). The cryptochromes: blue light photoreceptors in plants and animals. *Annu. Rev. Plant Biol.* **62**: 335–364.
- Duval, S., Danyal, K., Shaw, S., Lytle, A.K., Dean, D.R., Hoffman, B.M., Antony, E., and Seefeldt, L.C.** (2013). Electron transfer precedes ATP hydrolysis during nitrogenase catalysis. *Proc. Natl. Acad. Sci. USA* **110**: 16414–16419.
- Exner, V., Alexandre, C., Rosenfeldt, G., Alfarano, P., Nater, M., Caffisch, A., Gruissem, W., Batschauer, A., and Hennig, L.** (2010). A gain-of-function mutation of *Arabidopsis* cryptochrome1 promotes flowering. *Plant Physiol.* **154**: 1633–1645.
- Fontana, A., de Laureto, P.P., Spolaore, B., Frare, E., Picotti, P., and Zamboni, M.** (2004). Probing protein structure by limited proteolysis. *Acta Biochim. Pol.* **51**: 299–321.
- Gegear, R.J., Foley, L.E., Casselman, A., and Reppert, S.M.** (2010). Animal cryptochromes mediate magnetoreception by an unconventional photochemical mechanism. *Nature* **463**: 804–807.
- Giese, B.** (2002). Electron transfer in DNA. *Curr. Opin. Chem. Biol.* **6**: 612–618.
- Hennig, S.E., Goetzl, S., Jeoung, J.-H., Bommer, M., Lenzian, F., Hildebrandt, P., and Dobbek, H.** (2014). ATP-induced electron transfer by redox-selective partner recognition. *Nat. Commun.* **5**: 4626.
- Herbel, V., Orth, C., Wenzel, R., Ahmad, M., Bittl, R., and Batschauer, A.** (2013). Lifetimes of Arabidopsis cryptochrome signaling states *in vivo*. *Plant J.* **74**: 583–592.
- Hirota, T., et al.** (2012). Identification of small molecule activators of cryptochrome. *Science* **337**: 1094–1097.
- Hoang, N., Schleicher, E., Kacprzak, S., Bouly, J.P., Picot, M., Wu, W., Berndt, A., Wolf, E., Bittl, R., and Ahmad, M.** (2008). Human and *Drosophila* cryptochromes are light activated by flavin photo-reduction in living cells. *PLoS Biol.* **6**: e160.
- Immeln, D., Schlesinger, R., Heberle, J., and Kottke, T.** (2007). Blue light induces radical formation and autophosphorylation in the light-sensitive domain of *Chlamydomonas* cryptochrome. *J. Biol. Chem.* **282**: 21720–21728.
- Immeln, D., et al.** (2010). Photoreaction of plant and DASH cryptochromes probed by infrared spectroscopy: the neutral radical state of flavoproteins. *J. Physiol. Chem. B.* **14**, 17155–61.
- Kondoh, M., Shiraishi, C., Müller, P., Ahmad, M., Hitomi, K., Getzoff, E.D., and Terazima, M.** (2011). Light-induced conformational changes in full-length *Arabidopsis thaliana* cryptochrome. *J. Mol. Biol.* **413**: 128–137.
- Li, X., Wang, Q., Yu, X., Liu, H., Yang, H., Zhao, C., Liu, X., Tan, C., Klejnot, J., Zhong, D., and Lin, C.** (2011). *Arabidopsis* cryptochrome 2 (CRY2) functions by the photoactivation mechanism distinct from the tryptophan (trp) triad-dependent photoreduction. *Proc. Natl. Acad. Sci. USA* **108**: 20844–20849.
- Lin, C., and Todo, T.** (2005). The cryptochromes. *Genome Biol.* **6**: 220.
- Liu, B., Zuo, Z., Liu, H., Liu, X., and Lin, C.** (2011). Arabidopsis cryptochrome 1 interacts with SPA1 to suppress COP1 activity in response to blue light. *Genes Dev.* **25**: 1029–1034.
- Liu, H., Yu, X., Li, K., Klejnot, J., Yang, H., Lisiero, D., and Lin, C.** (2008). Photoexcited CRY2 interacts with CIB1 to regulate transcription and floral initiation in *Arabidopsis*. *Science* **322**: 1535–1539.
- Liu, Y., Li, X., Li, K., Liu, H., and Liu, C.** (2013). Multiple bHLH proteins form heterodimers to mediate cry2-dependent regulation of flowering time in Arabidopsis. *PLoS Genet.* **9**: e1003861.
- Müller, P., and Ahmad, M.** (2011). Light-activated cryptochrome reacts with molecular oxygen to form a flavin-superoxide radical pair consistent with magnetoreception. *J. Biol. Chem.* **286**: 21033–21040.
- Müller, P., Bouly, J.P., Hitomi, K., Balland, V., Getzoff, E.D., Ritz, T., and Brettel, K.** (2014). ATP binding turns plant cryptochrome into an efficient natural photoswitch. *Sci. Rep.* **4**: 5175.
- Muren, N.B., Olmon, E.D., and Barton, J.K.** (2012). Solution, surface, and single molecule platforms for the study of DNA-mediated charge transport. *Phys. Chem. Chem. Phys.* **14**: 13754–13771.
- Ozturk, N., Selby, C.P., Zhong, D., and Sancar, A.** (2014). Mechanism of photosignaling by *Drosophila* cryptochrome: role of the redox status of the flavin chromophore. *J. Biol. Chem.* **289**: 4634–4642.
- Ozturk, N., Selby, C.P., Annayev, Y., Zhong, D., and Sancar, A.** (2011). Reaction mechanism of *Drosophila* cryptochrome. *Proc. Natl. Acad. Sci. USA* **108**: 516–521.
- Ozturk, N., VanVickle-Chavez, S.J., Akileswaran, L., Van Gelder, R.N., and Sancar, A.** (2013). Ramshackle (Brwd3) promotes light-induced ubiquitylation of *Drosophila* Cryptochrome by DDB1-CUL4-ROC1 E3 ligase complex. *Proc. Natl. Acad. Sci. USA* **110**: 4980–4985.
- Oztürk, N., Song, S.H., Selby, C.P., and Sancar, A.** (2008). Animal type 1 cryptochromes. Analysis of the redox state of the flavin cofactor by site-directed mutagenesis. *J. Biol. Chem.* **283**: 3256–3263.
- Partch, C.L., Clarkson, M.W., Özgür, S., Lee, A.L., and Sancar, A.** (2005). Role of structural plasticity in signal transduction by the cryptochrome blue-light photoreceptor. *Biochemistry* **44**: 3795–3805.
- Sali, A., and Blundell, T.L.** (1993). Comparative protein modelling by satisfaction of spatial restraints. *J. Mol. Biol.* **234**: 779–815.

- Song, S.H., Oztürk, N., Denaro, T.R., Arat, N.O., Kao, Y.T., Zhu, H., Zhong, D., Reppert, S.M., and Sancar, A. (2007). Formation and function of flavin anion radical in cryptochrome 1 blue-light photoreceptor of monarch butterfly. *J. Biol. Chem.* **282**: 17608–17612.
- Vaidya, A.T., Top, D., Manahan, C.C., Tokuda, J.M., Zhang, S., Pollack, L., Young, M.W., and Crane, B.R. (2013). Flavin reduction activates *Drosophila* cryptochrome. *Proc. Natl. Acad. Sci. USA* **110**: 20455–20460.
- VanVickle-Chavez, S.J., and Van Gelder, R.N. (2007). Action spectrum of *Drosophila* cryptochrome. *J. Biol. Chem.* **282**: 10561–10566.
- Weidler, G., Zur Oven-Krockhaus, S., Heunemann, M., Orth, C., Schleifenbaum, F., Harter, K., Hoecker, U., and Batschauer, A. (2012). Degradation of *Arabidopsis* CRY2 is regulated by SPA proteins and phytochrome A. *Plant Cell* **24**: 2610–2623.
- Yang, H.Q., Wu, Y.J., Tang, R.H., Liu, D., Liu, Y., and Cashmore, A.R. (2000). The C termini of *Arabidopsis* cryptochromes mediate a constitutive light response. *Cell* **103**: 815–827.
- Yu, X., Sayegh, R., Maymon, M., Warpeha, K., Klejnot, J., Yang, H., Huang, J., Lee, J., Kaufman, L., and Lin, C. (2009). Formation of nuclear bodies of *Arabidopsis* CRY2 in response to blue light is associated with its blue light-dependent degradation. *Plant Cell* **21**: 118–130.
- Zeugner, A., Byrdin, M., Bouly, J.P., Bakrim, N., Giovani, B., Brettel, K., and Ahmad, M. (2005). Light-induced electron transfer in *Arabidopsis* cryptochrome-1 correlates with in vivo function. *J. Biol. Chem.* **280**: 19437–19440.
- Zuo, Z., Liu, H., Liu, B., Liu, X., and Lin, C. (2011). Blue light-dependent interaction of CRY2 with SPA1 regulates COP1 activity and floral initiation in *Arabidopsis*. *Curr. Biol.* **21**: 841–847.
- Zuo, Z.C., Meng, Y.Y., Yu, X.H., Zhang, Z.L., Feng, D.S., Sun, S.F., Liu, B., and Lin, C.T. (2012). A study of the blue-light-dependent phosphorylation, degradation, and photobody formation of *Arabidopsis* CRY2. *Mol. Plant.* **5**: 726–733.

Cellular Metabolites Enhance the Light Sensitivity of *Arabidopsis* Cryptochrome through Alternate Electron Transfer Pathways

Christopher Engelhard, Xuecong Wang, David Robles, Julia Moldt, Lars-Oliver Essen, Alfred Batschauer, Robert Bittl and Margaret Ahmad

Plant Cell 2014;26;4519-4531; originally published online November 26, 2014;
DOI 10.1105/tpc.114.129809

This information is current as of February 12, 2015

Supplemental Data	http://www.plantcell.org/content/suppl/2014/11/24/tpc.114.129809.DC1.html
References	This article cites 52 articles, 23 of which can be accessed free at: http://www.plantcell.org/content/26/11/4519.full.html#ref-list-1
Permissions	https://www.copyright.com/ccc/openurl.do?sid=pd_hw1532298X&issn=1532298X&WT.mc_id=pd_hw1532298X
eTOCs	Sign up for eTOCs at: http://www.plantcell.org/cgi/alerts/ctmain
CiteTrack Alerts	Sign up for CiteTrack Alerts at: http://www.plantcell.org/cgi/alerts/ctmain
Subscription Information	Subscription Information for <i>The Plant Cell</i> and <i>Plant Physiology</i> is available at: http://www.aspb.org/publications/subscriptions.cfm